Gas-Phase Vibrational Spectroscopy of the Hydrocarbon Cations l-C₃H⁺, HC₃H⁺, and c-C₃H₂⁺: Structures, Isomers, and the Influence of Ne-Tagging

Sandra Brünken,*[,†,‡] Filippo Lipparini,[§,∥] Alexander Stoffels,[‡,†] Pavol Jusko,[‡,⊥] Britta Redlich,[†] Jürgen Gauss,[§] and Stephan Schlemmer[‡]

†FELIX Laboratory, Institute for Molecules and Materials, Radboud University, Toernooiveld 7c, NL-6525ED Nijmegen, The Netherlands

‡I. Physikalisches Institut, Universität zu Köln, Zülpicher Str. 77, D-50937 Köln, Germany

§Institut für Physikalische Chemie, Johannes Gutenberg-Universität Mainz, Duesbergweg 10-14, D-55128 Mainz, Germany

∥Dipartimento di Chimica e Chimica Industriale, Università di Pisa, Via G. Moruzzi 13, I-56124 Pisa, Italy

Ⓢ *Supporting Information*

ABSTRACT: We report the first gas-phase vibrational spectra of the hydrocarbon ions C_3H^+ and $C_3H_2^+$. The ions were produced by electron impact ionization of allene. Vibrational spectra of the mass-selected ions tagged with Ne were recorded using infrared predissociation spectroscopy in a cryogenic ion trap instrument using the intense and widely tunable radiation of a free electron laser. Comparison of high-level quantum chemical calculations and resonant depletion measurements revealed that the C_3H^+ ion is exclusively formed in its most stable linear isomeric form, whereas two isomers were observed for $C_3H_2^+$. Bands of the energetically favored cyclic c-$C_3H_2^+$ are in excellent agreement with calculated anharmonic frequencies, whereas for the linear open-shell HCCCH⁺ ($^2\Pi_g$) a detailed theoretical description of the spectrum remains challenging because of Renner−Teller and spin−orbit interactions. Good agreement between theory and experiment, however, is observed for the frequencies of the stretching modes for which an anharmonic treatment was possible. In the case of linear l-C_3H^+, small but non-negligible effects of the attached Ne on the ion fundamental band positions and the overall spectrum were found.
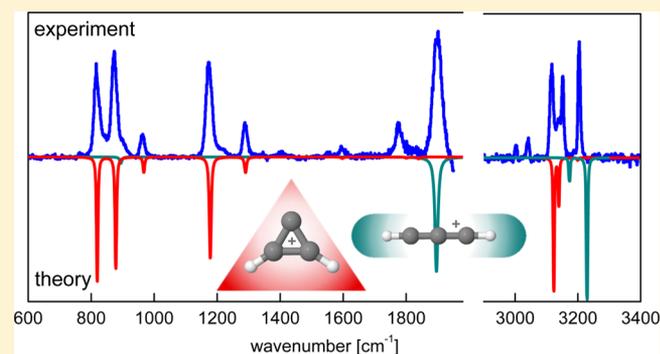
1. INTRODUCTION

The hydrocarbon ions C_3H^+ and $C_3H_2^+$ have long been recognized as important intermediates in the carbon chemistry in interstellar molecular clouds,[1,2] leading to the formation of ever more complex hydrocarbon chain molecules[3] and aromatic species such as benzene.[4] They are directly chemically related to the formation of the corresponding neutral species C_3H and C_3H_2, which are widespread in different regions in our Galaxy.[5−11] The dominant pathway leading to the neutrals is via dissociative electron recombination of $C_3H_2^+$ and $C_3H_3^+$, respectively, which in turn are formed via a competing reaction and association mechanism from C_3H^+ with H_2.[12] The latter reactions have been extensively studied in the laboratory at varying temperatures in selected ion flow tube (SIFT) and ion trap experiments, but still many open questions remain.[13−16] One of them is the role of isomeric variants of the reactant and product ions, all having stable cyclic and noncyclic forms, which can at best be indirectly probed by mass spectroscopic methods alone.[13] Isomer-dependent ion molecule reaction kinetics might be the

key to understand the large variation in the cyclic-to-linear isomer ratio of neutral C_3H_2 observed in different astronomical environments,[17,18] which is difficult to be reproduced in astrochemical model calculations.[19,20] Vibrational spectroscopy is a standard tool for structural determination. The IR data presented here on isomeric forms of C_3H^+ and $C_3H_2^+$ might, therefore, in future studies be used for probing the isomeric outcome of, for example, the astronomically relevant C_3H^+ + H_2 reaction.

The recent detection of the linear l-C_3H^+ isomer via its rotational transitions in several regions of the interstellar medium[11,21,22] has triggered several laboratory and theoretical spectroscopic studies on this closed-shell hydrocarbon ion. In order to identify the astronomical lines, high-resolution rotational spectra were recorded using rotational action spectroscopy in a cryogenic ion trap[23] and Fourier transform

microwave spectroscopy,[24] providing accurate spectroscopic parameters for its vibrational ground state. The observed large centrifugal distortion parameter prompted Huang et al.[25] to question the original identification of the astronomical lines as belonging to l-C_3H^+ based on quantum chemical calculations, resulting in a much smaller value. Later, further theoretical investigations resolved this issue and attributed the large centrifugal distortion effect to a shallow C−C−C bending potential in this linear ion, which is not accurately treated by the standard second-order vibrational perturbation theory (VPT2) approach.[26,27] However, to date, only indirect information on vibrational band positions of l-C_3H^+ is available from recent photoelectron spectroscopic studies.[28] In the same study, the cyclic c-C_3H^+ isomer was also observed, calculated to lie around 70 kJ/mol higher in energy than the linear isomeric ground state.[29]

The open-shell $C_3H_2^+$ ion has three stable isomers, with the cyclic (c-$C_3H_2^+$, $^2A_1$) variant being the ground state, followed by a linear $HCCCH^+$ ($^2\Pi_g$, 28 kJ/mol higher) and a linear C_{2v} ($^2A_1$, 182 kJ/mol higher) form. The relative energies are theoretical values, including zero-point energy corrections from Wong and Radom,[30] agreeing well with later calculations.[31] Experimental spectroscopic data on $C_3H_2^+$ are sparse. Franck−Condon analyses of the vibrationally resolved photoelectron spectra of neutral cyclic c-C_3H_2 provided estimates of the equilibrium geometry of cationic c-$C_3H_2^+$ and of its ν_2 and ν_3 stretching band positions.[32,33] In a more recent study, in addition, the threshold photoelectron spectrum of linear HCCCH was investigated for the first time.[28] Because this study aimed at determining adiabatic ionization energies of the neutrals, no information on the Renner−Teller-affected vibrational modes of $HCCCH^+$ was provided.

The combination of a cryogenic ion trap instrument with the widely tunable free electron lasers at the FELIX[a] Laboratory[34] enabled us now to measure the vibrational spectra of C_3H^+ and $C_3H_2^+$ for the first time. Broadband IR spectra covering most of the fundamental bands were recorded using infrared-predissociation (IR-PD) action spectroscopy of the isolated ions tagged with a Ne atom. The vibrational band positions are assigned and interpreted with the help of high-level quantum chemical calculations with an emphasis on the ions' isomeric composition and the influence of the rare gas tag.

2. EXPERIMENTAL AND THEORETICAL METHODS

2.1. FELion Cryogenic 22-Pole Ion Trap Instrument at the FELIX Laboratory.
The infrared spectra of linear C_3H^+ (propynylidynium) and two isomeric variants of $C_3H_2^+$ (the cyclic cyclopropenylidene and the linear radical cations) were recorded using the cryogenic 22-pole ion trap instrument FELion located at the Free Electron Lasers for Inrared eXperiments (FELIX) Laboratory at the Radboud University.[35] Details of the FELion instrument interfaced to the free electron laser FEL-2 at the FELIX Laboratory were given previously,[34] and here we will only provide information specific to the target ions and the employed action spectroscopic scheme, that is, IR-PD via Ne rare gas tagging.

C_3H^+ (m = 37 u) and $C_3H_2^+$ (m = 38 u) were produced in an ion storage source[36] from a mixture of neutral allene (propadiene, C_3H_4, 96%, abcr GmbH) and He at a ratio of 1:4 and pressure of $\sim 10^{-5}$ mbar via electron impact ionization at an energy of 20−30 eV. At the beginning of an experimental cycle, a 40−100 ms long pulse of ions is extracted from the source and filtered for the mass of interest by a first quadrupole

mass selector. The ions are guided to the 22-pole ion trap which is kept at a fixed temperature in the range 6.5−11.8 K, where they are cooled to the ambient temperature by collisions in a bath of He and Ne, with a mixture ratio of 3:1 and number density of $\sim 10^{15}$ cm^{-3}, provided via a pulsed piezo valve. The buffer gas pulse is triggered typically 10 ms before the ions enter the trap and continues until around 20−50 ms after the ion pulse. Under these conditions, around 10% of the primary ions (C_3H^+ or $C_3H_2^+$) form weakly bound complexes with Ne (see Figures S1 and S2 in the Supporting Information for corresponding mass spectra and time evolution).

For the spectroscopic experiments, the ions are stored for up to 7 s in the ion trap where they are exposed to several laser pulses before they are extracted from the trap. An IR-PD spectrum is recorded by mass-selecting and counting the C_3H^+-Ne (or $C_3H_2^+$-Ne) complex ions and varying the laser wavelength. The absorption of a resonant IR photon leads to a depletion in the number of complex ions $N(\nu)$ compared to the baseline number N_0 observed off-resonant. To account for saturation, varying baseline, laser pulse energy E, and pulse numbers n, the signal is normalized prior to averaging as $I = \frac{\ln(N(\nu)\,/\,N_0)}{n \cdot E\,/\,(h\nu)}$, yielding the intensity I in units of relative cross section per photon.

The IR radiation for the IR-PD measurements was provided by FEL-2 of the FELIX Laboratory (operated at 5 or 10 Hz) in the frequency region 500−1950 cm^{-1}. The macropulse energies in the interaction region were varied between 1 and 20 mJ, and the FEL optimized for narrow bandwidths of typically full width at half-maximum (fwhm) of 0.5−1 %. For C_3H^+, FEL-2 was also used in its third harmonic mode to cover the region 1950−2500 cm^{-1}. The CH stretching region between 2800 and 3900 cm^{-1} was covered with a tabletop OPO/OPA system (Laservision), providing 10 Hz pulsed IR radiation with up to 13 mJ/pulse and a fwhm of 3.5 cm^{-1}.

2.2. Quantum Chemical Calculations.
Quantum chemical calculations were performed to determine the structure and vibrational spectra of the species studied experimentally in this work. The structures of the ground states of C_3H^+ and cyclic c-$C_3H_2^+$ were optimized with analytical gradients at the coupled-cluster (CC) level of theory using the CC singles and doubles approximation[37] augmented with a perturbative treatment of triple excitations (CCSD(T)[38−40]). A restricted Hartree−Fock (HF) reference was used for the C_3H^+ ion, whereas an unrestricted HF (UHF) reference was employed for the open-shell c-$C_3H_2^+$ ion. The calculations were carried out using Dunning's cc-pCVQZ basis set[41] and with all electrons included in the correlation treatment. The stationary points found in the optimization were confirmed to be minima by computing analytical second derivatives.[42,43] The vibrational frequencies were determined at the same level of theory, including a treatment of anharmonicity based on VPT2.[44] Besides fundamental bands, the calculations allowed us to determine the presence of detectable overtones and combination bands, which allowed the assignment of additional peaks in the spectra. Our calculations are in good agreement with literature results[25−27] for C_3H^+ that, however, focus solely on fundamental bands and report no analysis of combination bands and overtones. To the best of our knowledge, this is the first report of high-level CC calculations of the vibrational frequencies for c-$C_3H_2^+$. Nevertheless, our results are in qualitative agreement with previous calculations[30] based on Møller−Plesset second-order perturbation theory.

For both species, the interaction with a noble gas atom was investigated computationally in order to understand the presence of stable complexes and the effect of the noble gas on the spectroscopic properties of the ions. For C_3H^+-Ne, we performed a scan of the C_3H^+-Ne potential energy surface by optimizing the distance between the neon atom and the central carbon upon varying the angle defined by the neon atom, the central carbon, and the hydrogen atom and by keeping every other geometrical parameter fixed. These calculations were first performed at the frozen-core (fc) CCSD(T)/aug-cc-pVTZ[45] level of theory, which allowed us to identify two potential stable complexes. Their geometries were further refined at the CCSD(T)/aug-cc-pCVQZ[41,45] level of theory, correlating all electrons. Harmonic frequencies were then computed at the same level of theory for both minima in order to confirm stability, and a transition state was optimized and confirmed again with a harmonic frequencies calculation, always at the CCSD(T)/aug-cc-pCVQZ level of theory. For c-$C_3H_2^+-Ne$, a two-dimensional scan was performed at the fc-CCSD(T)/cc-pVTZ level of theory. Three possible minima were identified, but further refinement of their geometries at the fc-CCSD(T)/aug-cc-pVTZ level of theory and harmonic frequencies calculations identified only a single minimum.

Computations were also carried out on the linear $HCCCH^+$ isomer. The electronic ground state of this ion is of $^2\Pi_g$ symmetry. While this state is, in principle, also accessible via single-reference CC theory, the instability of the UHF (as well as of a restricted open-shell HF) reference upon an antisymmetric stretch of the ion requires a different computational protocol. Furthermore, the computation of the vibrational spectrum requires to take into account the Renner–Teller splittings of the bending modes. We thus decided to use the equation-of-motion ionization potential[46] (EOMIP) CC approach, in which the $^2\Pi_g$ state is obtained by removing from the neutral triplet state of HCCCH an electron from one of the two singly occupied π orbitals. The main advantage of this approach is that one does not encounter any instability issues and that one is able to treat the Renner–Teller effect in its simplest variant. The geometry of $HCCCH^+$ was thus optimized at the EOMIP-CCSD[46] level of theory using the cc-pVQZ[47] basis set together with the fc approximation. Harmonic frequencies were computed for $HCCCH^+$ via numerical differentiation of analytically evaluated gradients,[46] resulting in two different values for each bending mode by following in one direction (e.g., x) the lower and in the other direction (e.g., y) the upper potential energy surface. For the anharmonic treatment, we refrain from a detailed handling of the Renner–Teller effect (as described, e.g., in ref 48) and focused solely on the stretching modes. This means that we report anharmonic results for stretching modes only, that is, their fundamentals, overtone and combination bands obtained by averaging the VPT2 results for both Renner–Teller components and ignoring all coupling contributions between both components.

Finally, for the sake of completeness, the structure and vibrational frequencies of a third, high-energy isomer of $C_3H_2^+$ with C_{2v} symmetry, that is, H_2CCC^+, were computed at the CCSD(T)/cc-pCVTZ level of theory.

All calculations were performed using the CFOUR suite of programs.[49] Detailed computational results can be found in the Supporting Information.

3. RESULTS AND DISCUSSION

3.1. Vibrational Spectrum of the Propynylidyne Ion, C_3H^+.
The IR-PD spectrum of the C_3H^+-Ne ion complex recorded in the cryogenic ion trap held at $T = 8.8$ K is displayed in Figure 1 (upper panel) and compares well to the
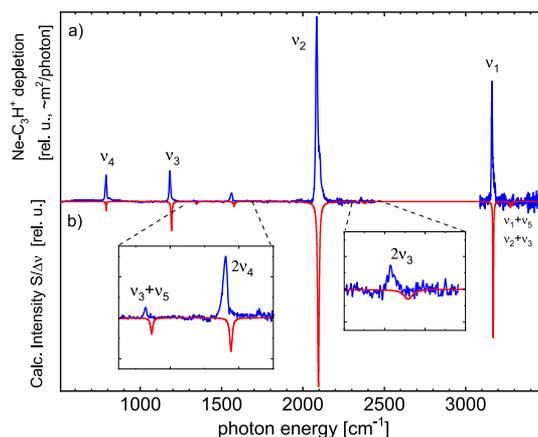

Figure 1. Vibrational spectrum of C_3H^+. (a) Experimental IR-PD spectrum of the C_3H^+-Ne complex recorded at $T = 8.8$ K in units of relative cross section. (b) Calculated band positions of bare linear C_3H^+ from anharmonic calculations at the CCSD(T)/cc-pCVQZ level of theory, folded with the corresponding laser line width.

calculated band positions of the untagged linear $^1\Sigma_g$ C_3H^+ ion (Figure 1 (lower panel) and Table 1). The measured fundamental bands corresponding to the H–C stretching (ν_1), the two C–C stretching (ν_2, ν_3), and the doubly degenerate H–C–C bending (ν_4) modes deviate by at most 10 cm^{-1} from the anharmonic (VPT2) calculations, whereas a substantially larger red shift (~20 cm^{-1}) is seen for the also observed weak $\nu_3 + \nu_5$, $2\nu_4$, and $2\nu_3$ combination and overtone bands. This is likely due to the shallow C–C–C bending (ν_5) potential discussed earlier,[27] which would require anharmonic corrections beyond the VPT2 level to accurately yield combination and overtone band positions. Nevertheless, such bands were assigned based on the results of the calculations. Whereas for the fundamental stretching bands our calculations agree well (within 2 cm^{-1}) with those presented earlier at higher level of theory,[25,26] for the same reason the ν_4 and ν_5 bending frequencies are overestimated in our calculations (by ~10 and 20 cm^{-1}, resp.). A comparison of harmonic and anharmonic calculations at the CCSD(T)/cc-pCVQZ level of theory and to earlier work is given in Tables S1 and S2 in the Supporting Information. Unfortunately, the ν_5 band position lies outside the accessible frequency range and could not be observed directly. The measured and calculated relative band intensities also agree remarkably well. This is not self-evident because in the experiment the signal strengths are a combination of the absorption cross section (i.e., the calculated band intensity) and the dissociation probability of the Ne–ion complex. The latter could well be mode-dependent, for example, because of different couplings to the dissociating modes involving the Ne–ion stretching and bending bands. The observed good match between theoretical and experimental values in the case of C_3H^+–Ne therefore indicates that the absorption of a single photon[b] leads to predissociation in nearly 100% of the cases, independent of the excited mode,

Table 1. Comparison of Experimental Ne-IR-PD Vibrational Band Positions and Calculated Anharmonic Frequencies and Intensities, Including Fundamental Frequencies and all Overtones and Combination Bands More Intense Than 0.1 km/mol up to 4000 cm^{-1}, for the Bare C_3H^+ Ion Computed at the CCSD(T)/cc-pCVQZ Level of Theory[a]

mode	IR-PD	rel. int.	fwhm	calc.	calc. int.
ν_5 (2)				135	71.6
$2\nu_5$ (2)				271	0.3
ν_4 (2)	789(2)	0.8	8	791	4.7
$\nu_4 + \nu_{Ne}$?	810(2)	0.1	15		
$\nu_4 + \nu_5$ (2)				926	0.1
ν_3	1182(2)	0.9	8	1192	73.1
$\nu_3 + \nu_{Ne}$?	1189(2)	0.1	34		
$\nu_3 + \nu_5$ (2)	1328(2)	0.05	8	1346	3.6
$2\nu_4$ (2)	1561(2)	0.2	8	1577	9.5
ν_2	2084(2)	4.8	9	2095	1174.4
$\nu_2 + \nu_{Ne}$?	2094(2)	1.9	29		
$\nu_2 + \nu_5$ (2)	2212(2)			2219	0.3
$2\nu_3$ (2)	2358(2)	0.1	8	2379	15.4
ν_1	3162(2)	3.3	6	3170*	109.4
ν_1 other Ne isomer?	3169(2)	1.1	17		
$\nu_1 + \nu_{Ne}$?	3181(2)				
$\nu_2 + \nu_3$				3276*	4.9
$\nu_1 + \nu_5$ (2)				3286	1.3
$\nu_1 + \nu_4$ (2)				3924	3.3

[a]Frequencies and widths in cm^{-1}, and calculated intensities in km/mol. Degenerate modes are marked with (2); tentative assignments are marked with "?"; lines marked with "*" belong to a Fermi resonance, which has been accounted for in the calculation. Experimental frequencies, widths, and intensities were obtained from multi-component Gaussian least-square fits.

Figure 2. Energy as a function of the X−C−H angle (X = He, Ne, Ar). The distance between the Ne atom and C_3H^+ was optimized at the CCSD(T)/cc-pVTZ level of theory for each value of the X−C−H angle.

and that the IR-PD spectrum can be taken as a proxy for the corresponding absorption spectrum.

The absence of additional vibrational features provides evidence that only the energetically lowest-lying linear C_3H^+ isomer is produced efficiently in our storage ion source from electron impact ionization of allene and that the formation of the 220 kJ mol^{-1} higher-lying cyclic isomer c-C_3H^+ is efficiently quenched, as has been observed in previous studies.[15,16,23]

Whereas IR-PD of tagged ions is commonly used to infer the spectra of the bare ions, in particular when using weakly bound rare gas atoms,[50−52] the attached rare gas atom does shift the observed band positions or induces splittings because of symmetry breaking.[53] Additionally, combination bands involving the low-lying stretching and bending modes of the attached atom generally lead to blue-shifted satellite features accompanying the fundamental bands.

In order to better understand the interaction of the neon atom with the ion and its effect on the vibrational spectrum, we performed a scan of the C_3H^+−Ne potential energy surface as described in Section 2.2. The same analysis was repeated for helium and argon; computations were carried out at the CCSD(T)/cc-pVTZ level of theory using the frozen-core approximation. The results, reported in Figure 2, show that there are two minima: a global one, corresponding to a linear structure with the rare gas atom close to the hydrogen atom, and a bent structure. For the Ne−ion complexes, the structures corresponding to both minima have been further optimized at the CCSD(T)/aug-cc-pCVQZ level of theory correlating all
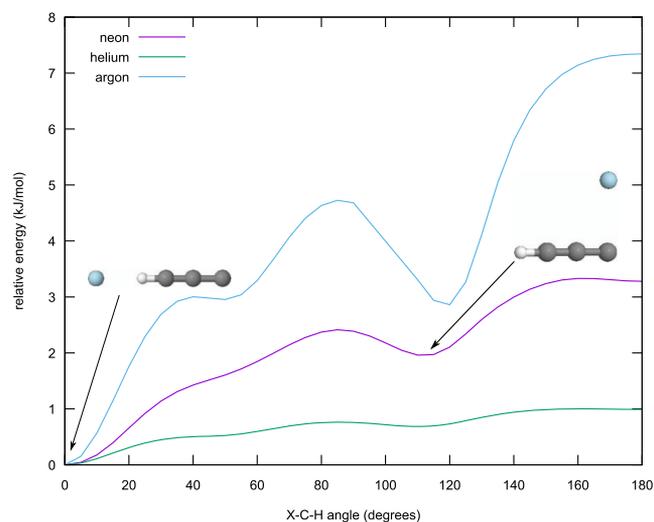
electrons and relaxing all geometrical parameters, and harmonic frequencies have been computed in order to estimate the shift because of the neon atom. The results are reported in Table 2. The transition state between the two minima was finally optimized at the same level of theory in order to have an estimate of the barrier heights. The barrier heights, computed as the energy difference between the transition state and the minima and including zero-point vibrational energy corrections, are 81 and 6 cm^{-1} for the linear-to-bent and bent-to-linear conversion, respectively. Details are reported in Section S2 of the Supporting Information.

The harmonic frequencies of Ne−ion vibrations of the complex given in Table 2 are of the order of several tens of cm^{-1}. We observed blue-shifted satellite features close to the ν_2, ν_3, and ν_4 bands in the measured spectrum. The corresponding peak positions obtained from a two-component Gaussian fit (see Supporting Information S7−S9) are also given in Table 1 and are assigned to combination bands of the C_3H^+ fundamental bands with the Ne−ion vibrations. These bands are significantly broader than the fundamental bands, whose line widths are given by the FEL's and OPO's instrumental line width, indicating a faster predissociation caused by the excitation of a mode coupled to the Ne dissociation coordinate. In order to exclude that the satellite features stem from unresolved rotational substructure, we have simulated the ro-vibrational spectrum for the ν_2 C−C stretch σ transition at 2084 cm^{-1} (with a forbidden Q-branch) and for the ν_4 C−C−H bending π transition at 789 cm^{-1}, exhibiting P-, Q-, and R-branch. The results of this simulation for $T = 12$ K using the calculated C_3H^+−Ne rotational ground-state constant of 1689 MHz (and ±1% change in the vibrational excited states) are shown in Figures S10 and S11 of the Supporting Information. They clearly show that the ro-vibrational structure cannot be resolved with the given instrumental bandwidth. Furthermore, in all cases, the R-branch is expected to be stronger than the P-branch, that is, resulting in a weaker red-shifted satellite, opposite to what is observed experimentally.

The values reported in Table 2 should provide a rough estimate of the shifts induced by the attached noble gas, which

Table 2. Harmonic Frequencies (in cm^{-1}) for the C$_3$H$^+$ Ion and the Two Complexes with Neon As Described in the Text Computed at the CCSD(T)/aug-cc-pCVQZ Level of Theory^a

mode	C$_3$H$^+$	C$_3$H$^+$−Ne	
		linear	bent
ν_7		35	
ν_7		35	28
ν_6		77	60
ν_5	130	133 (3)	125 (−5)
ν_5'	130	133 (3)	135 (5)
ν_4	803	820 (17)	800 (−3)
ν_4'	803	820 (17)	802 (−1)
ν_3	1187	1189 (2)	1188 (1)
ν_2	2139	2137 (−2)	2139 (0)
ν_1	3307	3294 (−13)	3308 (1)

^{a}The shifts are reported in parentheses. The frequencies labeled as ν_6 and ν_7 refer to the Ne−ion vibrations; the latter is doubly degenerate for the linear complex.

should be resolvable for the ν_1 and ν_4 vibrational bands. In order to further investigate this experimentally, we (i) recorded the ν_1 vibrational band again at a lower nominal trap temperature of $T = 6.5$ K and (ii) measured the saturation depletion behavior of this and other bands. For the latter measurements, the relative depletion $1 - N(\nu_i)/N_0$ at the peak band position ν_i of the tagged C$_3$H$^+$−Ne complexes is recorded as a function of total deposited energy $E \cdot n$ by varying either the irradiation time or the laser power. The interesting results of both measurements for the ν_1 band are shown in Figure 3. When lowering the trap temperature from $T = 10$ K to $T = 6.5$ K, the blue-shifted satellite disappears, and the maximum achievable depletion of the main peak increases from 70 to 100%. One possible explanation for this is the presence of a blue-shifted hot band involving a low-lying Ne vibration that is more populated at elevated temperatures. A more likely explanation is the formation of two structural C$_3$H$^+$−Ne isomers with a 7:3 abundance ratio at $T = 10$ K and effective quenching to only one structural isomer at $T = 6.5$ K. From a comparison of the calculated energy surface and isomeric shifts, we attribute the main peak to the lowest-lying linear C$_3$H$^+$−Ne isomer and the blue-shifted satellite (experimental shift of 7 cm^{-1}) to the bent isomer. For the ν_4 H−C−C bending mode, the situation is not very clear. Although the calculated large blue shift in the ν_4 mode of the linear isomer is not observed, we infer the presence of the red-shifted bent isomer from the observed broad (fwhm 300 cm^{-1}) and red-shifted (55 cm^{-1}) pedestal at this position (see Figure S7, Supporting Information). Fast predissociation, resulting in a broad band, can be expected for the bent isomer upon excitation of the bending mode because of its coupling with the dissociative Ne-stretching mode. Once again, anharmonic effects are expected to be more pronounced for the bending mode and absolute band positions and Ne-induced shifts are likely not well reproduced for the ν_4 mode at the current level of theory. We should also note that we were able to deplete the ν_3 band, which has a predicted small band shift between the two Ne−ion isomers less than the bandwidth, to 100% at the higher temperature conditions ($T = 8.8$ K). Thus, we can exclude experimental artifacts, such as a different overlap between the ion cloud and laser beam at different temper-
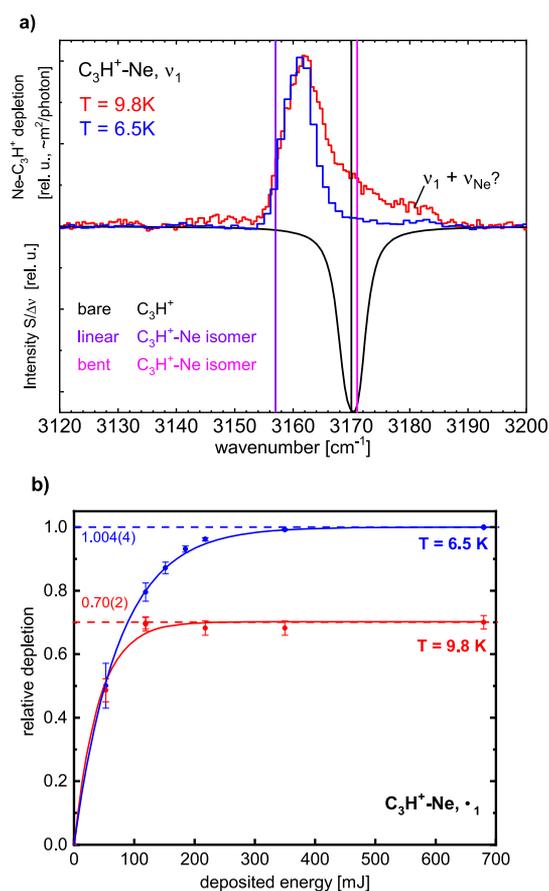

Figure 3. Existence of both C$_3$H$^+$−Ne isomers at elevated temperatures. (a) Upper panel: Comparison of the IR-PD spectrum of the ν_1 band recorded at $T = 6.5$ K and $T = 9.8$ K. Lower panel: Calculated anharmonic band position of C$_3$H$^+$ (folded with the laser line width) and calculated band positions of the linear and bent C$_3$H$^+$−Ne isomers (as sticks) based on the shifts reported in Table 2. (b) Relative depletion of the IR-PD signal at the $\nu_1 = 3162$ cm^{-1} peak position for both temperatures. The offset position was at 3140 cm^{-1}.

atures, to be responsible for the observed smaller depletion on the ν_1 band.

The existence of both C$_3$H$^+$-Ne isomers, while providing a possible explanation to the experimental results, is questionable because the computed barrier height including zero-point energies (energies are reported in Table S5) for the bent-to-linear conversion is only 6 cm^{-1} (linear-to-bent: 81 cm^{-1}). Whereas this would allow for a localized structure, one would expect efficient collisional cooling to the lowest energy isomer, with the population described by a Boltzmann distribution governed by the linear-to-bent barrier height. The experimental results indicate, however, that at slightly elevated temperatures a comparatively large fraction of the bent isomer is thermally populated, which might be caused by much smaller (of the order few cm^{-1}) barriers and energy differences than calculated. Additionally, more systematic experiments on the temperature dependence of the isomeric ratio are warranted to clarify the results.

3.2. Vibrational Spectra of the Linear and Cyclic Isomer of C$_3$H$_2^+$. The presence of two stable structural isomers of C$_3$H$_2^+$, the cyclopropenylidine ion (c-C$_3$H$_2^+$, ^{2}A$_1$) ground-state structure and a 28 kJ/mol higher-lying linear isomer (HCCCH$^+$, $^2\Pi$), has been inferred previously from SIFT reactivity studies,[13] photoelectron spectroscopy,[28] and

quantum chemical calculations.[30] Evidence for both isomers is present in our experimental IR-PD spectrum (shown in Figure 4) of Ne-tagged $C_3H_2^+$ produced by electron impact
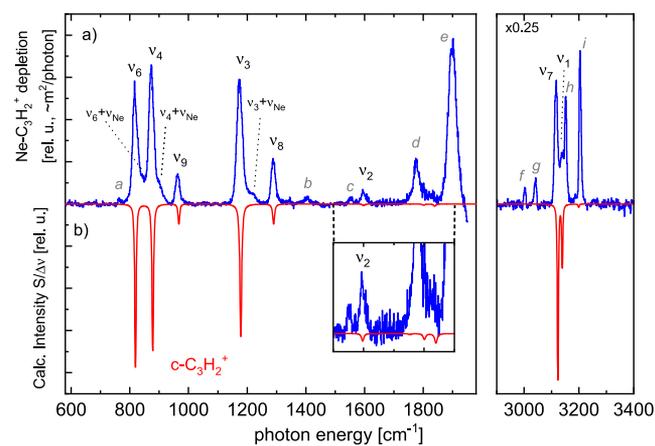

Figure 4. Vibrational spectrum of $C_3H_2^+$. (a) Experimental IR-PD spectrum of the $C_3H_2^+$-Ne complex recorded at $T = 7-10.5$ K in units of relative cross section. (b) Calculated band positions of bare (cyclic) c-$C_3H_2^+$ ($^2A_1$) from anharmonic calculations at the CCSD(T)/cc-pCVQZ level of theory, folded with the corresponding laser line width.

ionization of allene. Because no differences were found in the normalized spectra that were recorded using varying ionization energies (20−30 eV), irradiation power, different nominal trap temperatures ($T = 7-10.5$ K), and storage times, Figure 4 displays an average spectrum of all data.

From a comparison of calculated anharmonic band positions (Figure 4b), the majority of the strong bands can be assigned to the active fundamental vibrations of c-$C_3H_2^+$, $\nu_1-\nu_4$, and $\nu_6-\nu_9$. A summary of the assignment is given in Table 3. The agreement of the experimental c-$C_3H_2^+$−Ne vibrational frequencies to the calculated bare c-$C_3H_2^+$ band positions is excellent and in all cases better than 0.6%. From a potential energy surface scan, we determined the minimum structure of the ion−Ne complex as the one where the Ne atom lies in the molecular plane and on the C−H axis. The computational results for the induced band shift due to the attached Ne atom are given in Table 4, and the small effect of the attached Ne atom on the vibrational band positions is verified. Details of the computations are given in the Supporting Information. The fundamental bands of the ion−Ne vibrations are also given in Table 4, and we attribute the blue shoulders of the ν_6, ν_4, and ν_3 bands to combination bands involving these modes. The only previously reported vibrational frequencies for c-$C_3H_2^+$ stem from an analysis of vibrational progressions observed by threshold photoelectron spectroscopy of c-C_3H_2.[33] Their derived fundamental frequencies $\nu_3 = 1150(60)$ and $\nu_2 = 1530(60)$ are in reasonable agreement with our results.

Upon inspection of Figure 4, it is obvious that not all observed vibrational features can be attributed to c-$C_3H_2^+$. Moreover, the presence of a second isomer with the same molecular mass can be inferred from saturation depletion measurements which we performed on the strong ν_7, ν_8, ν_3, and ν_4 c-$C_3H_2^+$ bands. Only 60% of the stored complexes could be depleted at these resonant frequencies, whereas the bands labeled d, e, h, and i depleted by a maximum of 40%, indicating a 60:40 abundance ratio of the cyclic c-$C_3H_2^+$ to linear HCCCH$^+$ isomer if we assume that both ions have a

Table 3. Experimental IR-PD and Anharmonic Frequencies (in cm^1) and Intensities (in km/mol), Including Fundamental Frequencies and All Overtones and Combination Bands More Intense Than 0.1 km/mol up to 3900 cm^{-1}, for $C_3H_2^+$ (Cyclic Isomer), Computed at the CCSD(T)/cc-pCVQZ Level of Theory and by Using VPT2 for the Anharmonicity[a]

mode	IR-PD	rel. int.	fwhm	calc.	calc. int.
ν_6	819(2)	0.5	25	819	49.6
ν_4	873(2)	0.6	25	878	53.7
ν_9	963(2)	0.1	17	967	8.8
ν_5				983	0.0
ν_3	1174(2)	0.5	22	1178	79.7
$\nu3 + \nu_{Ne}$	1197(2)	0.1	57		
ν_8	1289(2)	0.2	18	1290	14.0
ν_2	1597(2)	0.05	23	1597*	1.8
$2\nu_6$				1640*	0.1
$2\nu_4$	1778(3) blend			1753	0.3
$\nu_5 + \nu_6$	1778(3) blend			1801	1.7
$\nu_4 + \nu_9$	1778(3) blend			1839	2.8
$2\nu_9$				1930	0.4
$2\nu_5$	nc			1964	0.2
$\nu_3 + \nu_4$	nc			2047	0.1
$\nu_4 + \nu_8$	nc			2176	0.1
$\nu_8 + \nu_9$	nc			2257	0.1
$2\nu_3$	nc			2339	0.4
$\nu_2 + \nu_6$	nc			2398	0.2
$\nu_3 + \nu_8$	nc			2468	0.4
$2\nu_8$	nc			2577	0.6
$\nu_2 + \nu_3$	nc			2766	0.3
$\nu_2 + \nu_8$				2879	1.3
ν_7	3116(2)	2.2	13	3123	136.4
ν_1	3139 (2)	0.9	23	3139*	48.3
$2\nu_2$	3204(2) blend			3199*	2.6

[a] Frequencies and widths in cm^{-1}, and calculated intensities in km/mol. "nc" means not covered experimentally; lines marked with "*" belong to a Fermi resonance, which has been accounted for in the calculation. Experimental frequencies, widths, and intensities were obtained from multi-component Gaussian least-square fits.

Table 4. Harmonic Frequencies (in cm^{-1}) for the $C_3H_2^+$ Ion and Its Stable Complex with Neon Described in the Text Computed at the fc-CCSD(T)/aug-cc-pVTZ Level of Theory[a]

mode	$C_3H_2^+$	$C_3H_2^+$−Ne
ν_{11}		34
ν_{10}		50
ν_9		75
ν_6	829	824 (−5)
ν_4	900	895 (5)
ν_9	986	981 (−5)
ν_5	994	989 (−5)
ν_3	1196	1196 (0)
ν_8	1305	1305 (0)
ν_2	1623	1622 (−1)
ν_7	3232	3230 (−2)
ν_1	3260	3258 (−2)

[a] The shifts are reported in parentheses. The frequencies labeled as ν_9, ν_{10}, and ν_{11} refer to the Ne−ion vibrations.

similar tagging efficiency. We can exclude the presence of the energetically high-lying (by 195 kJ/mol with respect to c-

Table 5. Experimental IR-PD Band Centers and Intensities of HCCCH⁺−Ne and Calculated Frequencies for the HCCCH⁺ Ion Computed at the fc-EOM-IP-CCSD/cc-pVQZ Level of Theory[a,b]

mode	symmetry	label	IR-PD	rel. int	fwhm	calc.	calc. int.
ν_7'	$\pi_u(y)$					208	55.6
ν_7	$\pi_u(x)$					279	28.8
ν_6'	$\pi_g(y)$					270	0.0
ν_6	$\pi_g(x)$					897	0.0
ν_5'	$\pi_u(y)$					385	61.6
ν_5	$\pi_u(x)$					894	10.6
		a	765(2)	0.02	10		
ν_2	σ_g^+					1301	0.0
		b	1403(2)	0.03	29		
		c	1554(2)	0.03	17		
		d	1778(2)	0.17	34		
ν_4	σ_u^-	e	1899(2)	0.75	33	1896	396.1
		f	3003(2)	0.34	7		
		g	3041(2)	0.46	9		
$\nu_2 + \nu_4$	σ_u^-	h	3152(2)	1.6	8	3173	45.2
ν_3	σ_u^-	i	3204(2)	2.9	9	3229	271.8
ν_1	σ_g^+					3360	0.0

[a]Harmonic frequencies are given for the Renner−Teller split modes, which are indicated with the same mode label, with and without apex, respectively. Anharmonic frequencies are given for the stretching bands, derived as the averages of the two Renner−Teller bending potentials. For details, see the Supporting Information. Labels a−i are referring to Figure 4. [b]Frequencies and widths in cm⁻¹, and calculated intensities in km/mol. Experimental frequencies, widths, and intensities were obtained from multi-component Gaussian least-square fits.

$C_3H_2^+$, as computed at the CCSD(T)/cc-pCVQZ level of theory) linear C_{2v} isomer based on a comparison of the experimental spectrum and calculated anharmonic band positions (see the Supporting Information); in particular, a predicted strong CC stretching band at 1133 cm⁻¹ is missing.

The electronic ground state of the linear HCCCH⁺ isomer is $^2\Pi_g$. Our results for the harmonic frequencies of the bending modes and the anharmonic frequencies for the stretching modes, as obtained at the fc-EOMIP-CCSD/cc-pVQZ level of theory, are given in Table 5, together with the experimental band positions labeled a−i in Figure 4. The strong active σ_u asymmetric stretching transitions ν_4 and ν_3 could be assigned, as well as an intense combination band of the symmetric and asymmetric CC stretching modes ($\nu_2 + \nu_4$). It should be noted that the computed frequencies of the Renner−Teller split[28] π modes are to be considered only qualitative estimates for the expected $\Delta - \Pi$ and $\Sigma - \Pi$ bending vibrational components because of the harmonic approximation and the lack of a proper treatment of the Renner−Teller effect as well as of spin−orbit coupling. Additionally, the attached Ne atom might introduce symmetry breaking depending on the most stable attachment position, thus also the symmetry-forbidden modes with gerade symmetry could be observable. Thus, the remaining unassigned bands are likely combination and overtone bands also belonging to the linear HCCCH⁺ isomer.

Apparently, the electron impact ionization of allene in the used ion storage source produces both the minimum cyclopropenylidine c-$C_3H_2^+$ and the higher-lying HCCCH⁺ isomer at the derived 60:40 ratio. The chosen electron impact energy of 20−30 eV is at least 5.6 eV higher than the appearance energy of 14.34(8) eV for $C_3H_2^+$ upon electron impact ionization of allene,[54] and the internal energy is thus sufficient to overcome the isomerization barriers of 182 kJ/mol (1.89 eV) and 408 kJ/mol (4.22 eV) from the linear to cyclic $C_3H_2^+$ forms and vice versa, respectively.[30] However, the isomeric ratio might have shifted in favor of the cyclic isomer via secondary reactions in our storage ion source because of

the higher reactivity of the linear isomer.[13] In the earlier SIFT measurements,[13] where propyne (CH₃CCH) was used as a precursor for $C_3H_2^+$ production via direct electron impact ionization, a ratio of 20:80 was found for the cyclic-to-linear isomer ratio.

4. CONCLUSIONS

This works presents the first gas-phase vibrational spectra of linear C_3H^+ and the two lowest isomers of $C_3H_2^+$ over a wide frequency range provided by the FELIX free electron lasers. The experimentally derived band positions for C_3H^+ and c-$C_3H_2^+$ are in excellent agreement with high-level quantum chemical calculations of the respective isomeric structures and corresponding anharmonic frequency calculations. Thanks to the interplay between theory and experiment, most of the spectral features of these ions could be assigned and, in the case of combination bands or overtones, calculations were able to guide the measurements, which confirmed the computational results. This in turn allows us to put strong constraints on the structural parameters of these ions.

The influence of the Ne atom attached to the molecular ions on vibrational band positions was investigated in detail with high-level quantum chemical calculations. In general, the deduced shifts were small, of the order of a few cm⁻¹, allowing for a clear assignment of vibrational modes of the bare ions from the experimental IR-PD spectra. The use of He as the tagging agent would introduce even smaller band shifts as discussed in previous studies[34,50,55] but was not applied here because of very low He attachment efficiencies (of the order of 1%). Nevertheless, subtle effects of the Ne tag were observable in the case of C_3H^+, which are challenging to interpret. On the other hand, this observation and the appearance of combination bands involving the Ne−ion bending and stretching modes can be turned into a tool to study the weak van der Waals interaction in the Ne−ion complexes.

The experimental and theoretical vibrational data presented here form a solid basis for further investigations of these ions at

higher resolution, for example, using the action spectroscopic method LIICG (laser-induced inhibition of complex growth) or LIR (laser-induced reactions). Both methods in combination with narrow-band IR excitation with a frequency-comb calibrated cw OPO were applied in the past successfully to record high-resolution ro-vibrational transitions of several other reactive ionic species, for example, CH_5^+, CH^+, and O_2H^+.[56−58] Ultimately, the goal would be to record directly the purely rotational transitions of c-$C_3H_2^+$ at highest precision. That this is possible even for reactive hydrocarbons has already been demonstrated in the case of linear C_3H^+. In fact, the latter ion was the first one for which the ROSAA (rotational state-dependent attachment of rare gas atoms) action spectroscopic method[59] was used to record its rotational spectrum, thereby confirming its detection in space.[23] Once the rotational fingerprint transitions of c-$C_3H_2^+$ are measured in the laboratory, they in turn will enable searches for this important intermediate in interstellar carbon chemistry using sensitive radio telescopes.

Vibrational IR-PD spectroscopy in combination with saturation depletion measurements, facilitated by the high FELIX FEL power, allows us to quantify the isomeric ratios of ions with a specific m/q value stored in our cryogenic ion trap, as described earlier[34,60] and applied here in the case of the $C_3H_2^+$ isomers. In future studies, we want to use these diagnostic capabilities to optimize the formation conditions of a specific isomer in the ion source. This in turn allows us to study subsequent ion molecule reactions starting with a well-defined isomer pure sample and to spectroscopically probe the product isomeric ratios, opening up new routes to reinvestigate the astronomically important C_3H^+ + H_2 reaction at low temperatures.[15,16,18]

Increasing the production yield of the linear $HCCCH^+$ isomer, for example, by using a propyne precursor or a nonstorage electron-impact ion source, will allow us to record its vibrational spectrum without possible blends with bands of the cyclic variant, thus enabling us to verify our tentative assignment of the stretching modes and to measure its low-lying Renner−Teller and spin−orbit disturbed bending modes. These data will provide an excellent basis to benchmark quantum chemical calculations, which are challenging for these linear open-shell species.

ASSOCIATED CONTENT

Ⓢ Supporting Information

The Supporting Information is available free of charge on the ACS Publications website at DOI: 10.1021/acs.jpca.9b06176.

> Mass spectra for ion production and complexation, details on the quantum chemical calculations, Gaussian fits to obtain experimental band positions, and simulations of the rotational contours (PDF)

AUTHOR INFORMATION

Corresponding Author

*E-mail: sandra.bruenken@ru.nl.

ORCID ⓞ

Sandra Brünken: 0000-0001-7175-4828

Filippo Lipparini: 0000-0002-4947-3912

Present Address

$^\perp$Max Planck Institute for Extraterrestrial Physics, Gießenbachstraße 1, 85748 Garching, Germany.

Notes

ADDITIONAL NOTES

^{a}Free electron lasers for infrared experiments, http://www.ru.nl/felix.

^{b}The Ne dissociation energy is 354 (235) cm^{-1} for the linear (bent) complex, which is well below the excitation energy of at least 550 cm^{-1} used in the presented experiments.

REFERENCES

(1) Herbst, E.; Adams, N. G.; Smith, D. Laboratory measurements of ion-molecule reactions pertaining to interstellar hydrocarbon synthesis. *Astrophys. J.* **1983**, *269*, 329−333.

(2) Smith, D. The ion chemistry of interstellar clouds. *Chem. Rev.* **1992**, *92*, 1473−1485.

(3) Turner, B. E.; Herbst, E.; Terzieva, R. The physics and chemistry of small translucent molecular clouds. XIII. The basic hydrocarbon chemistry. *Astrophys. J., Suppl. Ser.* **2000**, *126*, 427−460.

(4) McEwan, M. J.; Scott, G. B. I.; Adams, N. G.; Babcock, L. M.; Terzieva, R.; Herbst, E. New H and H_2 reactions with small hydrocarbon ions and their roles in benzene synthesis in dense interstellar clouds. *Astrophys. J.* **1999**, *513*, 287−293.

(5) Gottlieb, C. A.; Vrtilek, J. M.; Gottlieb, E. W.; Thaddeus, P.; Hjalmarson, A. Laboratory detection of the C_3H radical. *Astrophys. J.* **1985**, *294*, L55−L58.

(6) Thaddeus, P.; Gottlieb, C. A.; Hjalmarson, A.; Johansson, L. E. B.; Irvine, W. M.; Friberg, P.; Linke, R. A. Astronomical identification of the C_3H radical. *Astrophys. J.* **1985**, *294*, L49−L53.

(7) Yamamoto, S.; Saito, S.; Ohishi, M.; Suzuki, H.; Ishikawa, S.-I.; Kaifu, N.; Murakami, A. Laboratory and astronomical detection of the cyclic C_3H radical. *Astrophys. J.* **1987**, *322*, L55−L58.

(8) Cernicharo, J.; Gottlieb, C. A.; Guelin, M.; Killian, T. C.; Thaddeus, P.; Vrtilek, J. M.; Vrtilek, J. Astronomical detection of H_2CCC. *Astrophys. J.* **1991**, *368*, L43−L41.

(9) Cernicharo, J.; Cox, P.; Fosse, D.; Güsten, R. Detection of linear C_3H_2 in absorption toward continuum sources. *Astron. Astrophys.* **1999**, *351*, 341−346.

(10) Fosse, D.; Cernicharo, J.; Gerin, M.; Cox, P. Molecular Carbon Chains and Rings in TMC-1. *Astrophys. J.* **2001**, *552*, 168−174.

(11) Pety, J.; Gratier, P.; Guzmán, V.; Roueff, E.; Gerin, M.; Goicoechea, J. R.; Bardeau, S.; Sievers, A.; Le Petit, F.; Le Bourlot, J.; et al. The IRAM-30 m line survey of the Horsehead PDR. II. First detection of the l-C_3H^+ hydrocarbon cation. *Astron. Astrophys.* **2012**, *548*, A68.

(12) Maluendes, S. A.; Mclean, A. D.; Yamashita, K.; Herbst, E. Calculations on the competition between association and reaction for $C_3H^{++}H_2$. *J. Chem. Phys.* **1993**, *99*, 2812−2820.

(13) Smith, D.; Adams, N. G. Cyclic and linear isomers of C_3H2+ and C_3H3+ - the C3H+ + H2 reaction. *Int. J. Mass Spectrom.* **1987**, *76*, 307−317.

(14) Sorgenfrei, A.; Gerlich, D. Ion-trap experiments on $C_3H_++H_2$: radiative association vs. hydrogen abstraction. In *Physical Chemistry of Molecules and Grains in Space*; Nenner, I., Ed.; AIP Press: New York, 1994; pp 505−513.

(15) Savić, I.; Schlemmer, S.; Gerlich, D. Low-temperature experiments on the formation of deuterated $C_3H_3^+$. *Astrophys. J.* **2005**, *621*, 1163−1170.

(16) Savić, I.; Gerlich, D. Temperature variable ion trap studies of $C_3H_n^+$ with H_2 and HD. *Phys. Chem. Chem. Phys.* **2005**, *7*, 1026−1035.

(17) Spezzano, S.; Gupta, H.; Brünken, S.; Gottlieb, C. A.; Caselli, P.; Menten, K. M.; Mueller, H. S. P.; Bizzocchi, L.; Schilke, P.; McCarthy, M. C.; et al. A study of the C_3H_2 isomers and isotopologues: first interstellar detection of HDCCC. *Astron. Astrophys.* **2016**, *586*, A110.

(18) Loison, J.-C.; Agúndez, M.; Wakelam, V.; Roueff, E.; Gratier, P.; Marcelino, N.; Reyes, D. N.; Cernicharo, J.; Gerin, M. The interstellar chemistry of C_3H and C_3H_2 isomers. *Mon. Not. R. Astron. Soc.* **2017**, *470*, 4075−4088.

(19) Agúndez, M.; Wakelam, V. Chemistry of dark clouds: databases, networks, and models. *Chem. Rev.* **2013**, *113*, 8710−8737.

(20) Sipilä, O.; Spezzano, S.; Caselli, P. Understanding the C_3H_2 cyclic-to-linear ratio in L1544. *Astron. Astrophys.* **2016**, *591*, L1.

(21) McGuire, B. A.; Carroll, P. B.; Loomis, R. A.; Blake, G. A.; Hollis, J. M.; Lovas, F. J.; Jewell, P. R.; Remijan, A. J. A Search for l-C_3H^+ and l-C_3H in Sgr B2(N), Sgr B2(OH), and the Dark Cloud TMC-1. *Astrophys. J.* **2013**, *774*, 56.

(22) McGuire, B. A.; Carroll, P. B.; Sanders, J. L., III; Weaver, S. L. W.; Blake, G. A.; Remijan, A. J. A CSO search for l-C_3H^+: detection in the Orion Bar PDR. *Mon. Not. R. Astron. Soc.* **2014**, *442*, 2901−2908.

(23) Brünken, S.; Kluge, L.; Stoffels, A.; Asvany, O.; Schlemmer, S. Laboratory rotational spectrum of l-C_3H^+ and confirmation of its astronomical detection. *Astrophys. J.* **2014**, *783*, L4.

(24) McCarthy, M. C.; Crabtree, K. N.; Martin-Drumel, M.-A.; Martinez, O., Jr.; McGuire, B. A.; Gottlieb, C. A. A laboratory study of C_3H^+ and the C_3H radical in three new vibrationally excited Σ_2 states using a pin-hole nozzle discharge source. *Astrophys. J., Suppl. Ser.* **2015**, *217*, 10.

(25) Huang, X.; Fortenberry, R. C.; Lee, T. J. Spectroscopic constants and vibrational frequencies for l-C_3H^+ and isotopologues from highly accurate quartic force fields: the detection of l-C_3H^+ in the Horsehead nebula PDR questioned. *Astrophys. J.* **2013**, *768*, L25.

(26) Mladenović, M. The B11244 story: Rovibrational calculations for C_3H^+ and C_3H^- revisited. *J. Chem. Phys.* **2014**, *141*, 224304.

(27) Botschwina, P.; Stein, C.; Sebald, P.; Schröder, B.; Oswald, R. Strong theoretical support for the assignment of B11244 to l-C_3H^+. *Astrophys. J.* **2014**, *787*, 72.

(28) Garcia, G. A.; Gans, B.; Krüger, J.; Holzmeier, F.; Röder, A.; Lopes, A.; Fittschen, C.; Alcaraz, C.; Loison, J.-C. Valence shell threshold photoelectron spectroscopy of C_3H_x (x=0-3). *Phys. Chem. Chem. Phys.* **2018**, *20*, 8707−8718.

(29) Wang, Y.; Braams, B. J.; Bowman, J. M. Ab intio based potential energy surfaces and Franck-Condon analysis of ionization thresholds of cyclic-C_3H and linear-C_3H. *J. Phys. Chem. A* **2007**, *111*, 4056−4061.

(30) Wong, M. W.; Radom, L. Thermochemistry and ion-molecule reactions of isomeric C_3H^{2+} cations. *J. Am. Chem. Soc.* **1993**, *115*, 1507−1514.

(31) Holzmeier, F.; Fischer, I.; Kiendl, B.; Krueger, A.; Bodi, A.; Hemberger, P. On the absolute photoionization cross section and dissociative photoionization of cyclopropenylidene. *Phys. Chem. Chem. Phys.* **2016**, *18*, 9240−9247.

(32) Clauberg, H.; Chen, P. Geometry of c-C_3H^{2+} - Franck-Condon factors in photoionization are a sensitive probe of polyatomic ion structure. *J. Phys. Chem.* **1992**, *96*, 5676−5678.

(33) Hemberger, P.; Noller, B.; Steinbauer, M.; Fischer, I.; Alcaraz, C.; Cunha de Miranda, B. K.; Garcia, G. A.; Soldi-Lose, H. Threshold Photoelectron Spectroscopy of Cyclopropenylidene, Chlorocyclopropenylidene, and Their Deuterated Isotopomeres†. *J. Phys. Chem. A* **2010**, *114*, 11269−11276.

(34) Jusko, P.; Brünken, S.; Asvany, O.; Thorwirth, S.; Stoffels, A.; van der Meer, L.; Berden, G.; Redlich, B.; Oomens, J.; Schlemmer, S. The FELion cryogenic ion trap beam line at the FELIX free-electron laser laboratory: Infrared signatures of primary alcohol cations. *Faraday Discuss.* **2019**, *217*, 172−202.

(35) Oepts, D.; van der Meer, A. F. G.; van Amersfoort, P. W. The Free-Electron-Laser user facility FELIX. *Infrared Phys. Technol.* **1995**, *36*, 297−308.

(36) Gerlich, D. Inhomogeneous RF fields: a versatile tool for the study of processes with slow ions. In *Advances in Chemical Physics: State-Selected and State-to-State Ion-Molecule Reaction Dynamics*; Ng, C.-Y., Baer, M., Eds.; Wiley: New York, 1992; Vol. *LXXXII*, pp 1−176.

(37) Purvis, G. D.; Bartlett, R. J. A full coupled-cluster singles and doubles model: The inclusion of disconnected triples. *J. Chem. Phys.* **1982**, *76*, 1910−1918.

(38) Raghavachari, K.; Trucks, G. W.; Pople, J. A.; Head-Gordon, M. A fifth-order perturbation comparison of electron correlation theories. *Chem. Phys. Lett.* **1989**, *157*, 479−483.

(39) Scuseria, G. E. Analytic evaluation of energy gradients for the singles and doubles coupled cluster method including perturbative triple excitations: Theory and applications to FOOF and Cr_2. *J. Chem. Phys.* **1991**, *94*, 442−447.

(40) Watts, J. D.; Gauss, J.; Bartlett, R. J. Open-shell analytical energy gradients for triple excitation many-body, coupled-cluster methods: MBPT(4), CCSD+T(CCSD), CCSD(T),and QCISD(T). *Chem. Phys. Lett.* **1992**, *200*, 1−7.

(41) Woon, D. E.; Dunning, T. H. Gaussian basis sets for use in correlated molecular calculations. V. Core-valence basis sets for boron through neon. *J. Chem. Phys.* **1995**, *103*, 4572−4585.

(42) Gauss, J.; Stanton, J. F. Analytic CCSD(T) second derivatives. *Chem. Phys. Lett.* **1997**, *276*, 70−77.

(43) Szalay, P. G.; Gauss, J.; Stanton, J. F. Analytic UHF-CCSD(T) second derivatives: implementation and application to the calculation of the vibration-rotation interaction constants of NCO and NCS. *Theor. Chem. Acc. Theory Comput. Model.* **1998**, *100*, 5−11.

(44) Mills, I. M. In *Molecular Spectroscopy: Modern Research*; Narahari Rao, K., Mathews, C. W., Eds.; Academic Press: New York, 1977; Vol. *1*; pp 115−140.

(45) Kendall, R. A.; Dunning, T. H.; Harrison, R. J. Electron affinities of the first-row atoms revisited. Systematic basis sets and wave functions. *J. Chem. Phys.* **1992**, *96*, 6796−6806.

(46) Stanton, J. F.; Gauss, J. Analytic energy derivatives for ionized states described by the equation-of-motion coupled cluster method. *J. Chem. Phys.* **1994**, *101*, 8938−8944.

(47) Dunning, T. H. Gaussian basis sets for use in correlated molecular calculations. I. The atoms boron through neon and hydrogen. *J. Chem. Phys.* **1989**, *90*, 1007−1023.

(48) Perić, M.; Petković, M.; Jerosimić, S. Renner−Teller effect in five-atomic molecules: Ab initio investigation of the spectrum of C_5^-. *Chem. Phys.* **2008**, *343*, 141−157.

(49) Stanton, J. F.; Gauss, J.; Cheng, L.; Harding, M. E.; Matthews, D. A.; Szalay, P. G. CFOUR, Coupled-Cluster techniques for Computational Chemistry, a quantum-chemical program package. With contributions from Auer, A. A.; Bartlett, R. J.; Benedikt, U.; Berger, C.; Bernholdt, D. E.; Bomble, Y. J.; Christiansen, O.; Engel, F.; Faber, R.; Heckert, M.; Heun, O.; Hilgenberg, M.; Huber, C.; Jagau, T.-C.; Jonsson, D.; Jusélius, J.; Kirsch, T.; Klein, K.; Lauderdale, W. J.; Lipparini, F.; Metzroth, T.; Mück, L. A.; O'Neill, D. P.; Price, D. R.; Prochnow, E.; Puzzarini, C.; Ruud, K.; Schiffmann, F.; Schwalbach, W.; Simmons, C.; Stopkowicz, S.; Tajti, A.; Vázquez, J.; Wang, F.; Watts, J. D. and the integral packages MOLECULE (Almlöf, J.; Taylor, P. R.), PROPS (Taylor, P. R.), ABACUS (Helgaker, T.; Jensen, H. J. A.; Jørgensen, P.; Olsen, J.), and ECP routines (Mitinv, A. V.; van Wüllen, C.). For the current version, see http://www.cfour.de.

(50) Brümmer, M.; Kaposta, C.; Santambrogio, G.; Asmis, K. R. Formation and photodepletion of cluster ion−messenger atom complexes in a cold ion trap: Infrared spectroscopy of VO^+, VO_2^+, and VO_3^+. *J. Chem. Phys.* **2003**, *119*, 12700−12703.

(51) Duncan, M. A. Infrared Laser Spectroscopy of Mass-Selected Carbocations. *J. Phys. Chem. A* **2012**, *116*, 11477−11491.

(52) Roithová, J.; Gray, A.; Andris, E.; Jašík, J.; Gerlich, D. Helium Tagging Infrared Photodissociation Spectroscopy of Reactive Ions. *Acc. Chem. Res.* **2016**, *49*, 223−230.

(53) Schwarz, H.; Asmis, K. R. Identification of Active Sites and Structural Characterization of Reactive Ionic Intermediates by Cryogenic Ion Trap Vibrational Spectroscopy. *Chem.—Eur. J.* **2019**, *25*, 2112−2126.

(54) Franklin, J. L.; Mogenis, A. Electron impact study of ions from several dienes. *J. Phys. Chem.* **1967**, *71*, 2820−2824.

(55) Jašík, J.; Žabka, J.; Roithová, J.; Gerlich, D. Infrared spectroscopy of trapped molecular dications below 4 K. *Int. J. Mass Spectrom.* **2013**, *354−355*, 204−210.

(56) Asvany, O.; Yamada, K. M. T.; Brunken, S.; Potapov, A.; Schlemmer, S. Experimental ground-state combination differences of CH_5^+. *Science* **2015**, *347*, 1346−1349.

(57) Doménech, J. L.; Jusko, P.; Schlemmer, S.; Asvany, O. The First Laboratory detection of vibration-rotation transitions of $^{12}CH^+$ and $^{13}CH^+$ and improved measurement of their rotational transition frequencies. *Astrophys. J.* **2018**, *857*, 61.

(58) Kohguchi, H.; Jusko, P.; Yamada, K. M. T.; Schlemmer, S.; Asvany, O. High-resolution infrared spectroscopy of O2H+ in a cryogenic ion trap. *J. Chem. Phys.* **2018**, *148*, 144303.

(59) Brünken, S.; Kluge, L.; Stoffels, A.; Pérez-Ríos, J.; Schlemmer, S. Rotational state-dependent attachment of He atoms to cold molecular ions: An action spectroscopic scheme for rotational spectroscopy. *J. Mol. Spectrosc.* **2017**, *332*, 67−78.

(60) Jusko, P.; Simon, A.; Banhatti, S.; Brünken, S.; Joblin, C. Direct evidence of the benzylium and tropylium cations as the two long-lived isomers of $C_7H_7^+$. *ChemPhysChem* **2018**, *19*, 3182−3185.